

Light Scalar Mesons $\sigma(500)$, $f_0(980)$ and κ in Charm Meson Decays ¹

Ignacio Bediaga

Representing the Fermilab E791 Collaboration

Centro Brasileiro de Pesquisas Físicas,
Rua Xavier Sigaud 150, 22290, Rio de Janeiro, Brazil
bediaga@cbpf.br

Abstract

We present recent results on scalar light mesons based on Dalitz plot analyses of charm decays from Fermilab experiment E791. Scalar mesons are found to have large contributions to the decays studied, $D^+ \rightarrow K^-\pi^+\pi^+$ and $D^+, D_s^+ \rightarrow \pi^-\pi^+\pi^+$. From the first decay, we find good evidence for the existence of the light and broad κ meson and we measure its mass and width. We find strong evidence for the $\sigma(500)$ meson from $D^+ \rightarrow \pi^-\pi^+\pi^+$ decay and measure its mass and width. We also present the results obtained for the $f_0(980)$ parameters through the $D_s^+ \rightarrow \pi^-\pi^+\pi^+$ decay. These results demonstrate the importance of charm decays as a new environment for the study of light meson physics.

1 Introduction

The decays of charm mesons are currently a new source of information for the study of light meson spectroscopy, with the advantages of having well defined initial state (the D meson, a 0^- state with defined mass). This new information is complementary to that from scattering experiments and can be particularly relevant to the understanding of the scalar sector, due to the well-known difficulties of scattering experiments to observe light and broad scalar resonances.

Here we present an overview of the results we obtained analysing the decays $D_s^+ \rightarrow \pi^-\pi^+\pi^+$ [1], $D^+ \rightarrow \pi^-\pi^+\pi^+$ [2] and $D^+ \rightarrow K^-\pi^+\pi^+$ [3], using data collected in 1991/92 by Fermilab experiment E791 from 500 GeV/c π^- -nucleon interactions. For details see [4].

For the $D^+ \rightarrow \pi^-\pi^+\pi^+$ decays, we find that a model with only known $\pi\pi$ resonances plus a non-resonant (NR) channel is not able to describe the data adequately.

¹To appear in proceedings of VIII International Workshop on Hadron Physics 2002
Rio Grande do Sul, Brazil. World Scientific edition.

Thus we include a new amplitude in our fit function and find strong evidence for the presence of a light and broad scalar resonance, the $\sigma(500)$. The channel involving this scalar meson is responsible for half of the decay rate. We measure the mass and the width of this scalar meson to be $478^{+24}_{-23} \pm 17$ MeV/c² and $324^{+42}_{-40} \pm 21$ MeV/c², respectively. Other experiments have presented controversial evidence for this low-mass $\pi\pi$ resonance in partial wave analyses [5, 6, 7], with ambiguous interpretations of the characteristics of such particles[8, 9].

We found a similar situation for the $D^+ \rightarrow K^-\pi^+\pi^+$ analysis. When we include all known $K\pi$ resonant channels plus a NR contribution, we find that this model is not able to describe the data. By including an extra scalar resonant state, with unconstrained mass and width, we obtain a fit which is substantially superior to that without this state. The values for its mass and width are found to be $797 \pm 19 \pm 42$ MeV/c² and $410 \pm 43 \pm 85$ MeV/c² respectively. We refer to this state as the κ . We also obtain new measurements for the mass and the width of the $K_0^*(1430)$ resonance.

From our analysis of $D_s^+ \rightarrow \pi^-\pi^+\pi^+$ decays we found that the isoscalar intermediate states are dominant in this decay as well. The largest contribution to this final state comes from the decay involving the scalar meson $f_0(980)$ whose nature is a long-standing puzzle. It has been described as a $q\bar{q}$ state , a $K\bar{K}$ molecule, a glueball, and a multiquark state [8, 9]. We obtain new measurements for the $f_0(980)$ and $f_0(1370)$ masses and widths.

To obtain these results, we had to introduce a new approach in Dalitz plot analysis in order to extract the mass and width of the scalar resonances by using them as floating parameters in the fit. We begin this paper presenting the general method, applied in the $D^+ \rightarrow K^-\pi^+\pi^+$ Dalitz-plot analysis, then we discuss the $D_s^+ \rightarrow \pi^-\pi^+\pi^+$ and $D^+ \rightarrow \pi^-\pi^+\pi^+$ studies using the same procedure.

2 The $D^+ \rightarrow K^-\pi^+\pi^+$ Dalitz-plot Analysis

From the original 2×10^{10} events collected by E791, and after reconstruction and selection criteria, we obtained the $D^+ \rightarrow K^-\pi^+\pi^+$ sample shown in Figure 1(a). The filled area represents the level of background; besides the combinatorial, the other main source of background comes from the reflection of the decay $D_s^+ \rightarrow K^-K^+\pi^+$ (through \bar{K}^*K^+ and $\phi\pi^+$). The cross-hatched region contains the events selected for the Dalitz-plot analysis. There are 15090 events in this sample, of which 6% are background.

Figure 1(b) shows the Dalitz-plot for these events. The two axes are the squared invariant-mass combinations for $K\pi$, and the plot is symmetrized with respect to the two identical pions. The plot presents a rich structure, where we can observe the clear bands from $\bar{K}^*(890)\pi^+$, and an accumulation of events at the upper edge of the diagonal, due to heavier resonances. To study the resonant substructure, we perform an

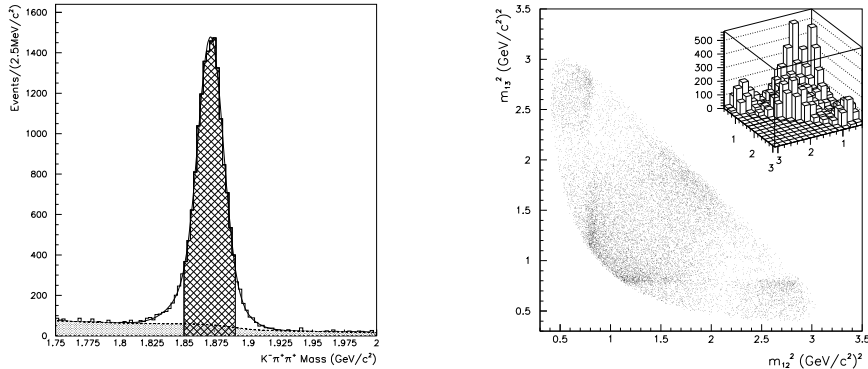


Figure 1: (a) The $K^- \pi^+ \pi^+$ invariant mass spectrum. The filled area is background; (b) Dalitz plot corresponding to the events in the cross-hatched area of (a).

unbinned maximum-likelihood fit to the data, with probability distribution functions (PDF's) for both signal and background sources. In particular, for each candidate event, the signal PDF is written as the square of the total physical amplitude \mathcal{A} and it is weighted for the acceptance across the Dalitz plot (obtained by Monte Carlo (MC)) and by the level of signal to background for each event, as given by the line shape of Figure 1(a). The background PDF's (levels and shapes) are fixed for the Dalitz-plot fit, according to MC and data studies.

We begin describing our first approach to fit the data, which represents the conventional Dalitz-plot analysis including the known $K\pi$ resonant amplitudes (\mathcal{A}_n , $n \geq 1$), plus a constant non-resonant contribution. The signal amplitude, a Breit-Wigner parametrization times a Blatt-Weisskopf damping factor, is described in reference [3].

Using this model with well-known resonances (Model A), we find contributions from the following channels: the non-resonant, responsible for more than 90% of the decay rate, followed by $\bar{K}_0^*(1430)\pi^+$, $\bar{K}^*(892)\pi^+$, $\bar{K}^*(1680)\pi^+$ and $\bar{K}_2^*(1430)\pi^+$. The decay fractions and relative phases are shown in Table 1. These values are in accordance with previous results from E691 [10] and E687 [11]. We thus confirm a high non-resonant contribution according to this model, which is totally unusual in D decays. Besides, there is an important destructive interference pattern, since all fractions add up to 140 %.

To evaluate the fit quality, we compute a χ^2 from binned, two-dimensional distributions of data and decay model events. The χ^2 comes from the differences in the binned numbers of events between the data and the model (from a fast MC simulation). We obtain $\chi^2/\nu = 2.7$ (ν being the number of degrees of freedom), with a corresponding confidence level (CL) of 10^{-11} . In Figure 2(a) we show the $K\pi$ low and high squared-mass projections for data (error bars) and model (solid line). The discrepancies are evident in the very low-mass region for $m^2(K\pi)_{low}$ and near 2.5

Decay Mode	Model A: No κ		Model B: With κ	
	Fraction (%)	Phase	Fraction (%)	Phase
NR	90.9 ± 2.6	0° (fixed)	$13.0 \pm 5.8 \pm 2.6$	$(349 \pm 14 \pm 8)^\circ$
$\kappa\pi^+$	—	—	$47.8 \pm 12.1 \pm 3.7$	$(187 \pm 8 \pm 17)^\circ$
$\bar{K}^*(892)\pi^+$	13.8 ± 0.5	$(54 \pm 2)^\circ$	$12.3 \pm 1.0 \pm 0.9$	0° (fixed)
$\bar{K}_0^*(1430)\pi^+$	30.6 ± 1.6	$(54 \pm 2)^\circ$	$12.5 \pm 1.4 \pm 0.4$	$(48 \pm 7 \pm 10)^\circ$
$\bar{K}_2^*(1430)\pi^+$	0.4 ± 0.1	$(33 \pm 8)^\circ$	$0.5 \pm 0.1 \pm 0.2$	$(306 \pm 8 \pm 6)^\circ$
$\bar{K}^*(1680)\pi^+$	3.2 ± 0.3	$(66 \pm 3)^\circ$	$2.5 \pm 0.7 \pm 0.2$	$(28 \pm 13 \pm 15)^\circ$

Table 1: Results without κ (Model A) and with κ (Model B).

$(\text{GeV}/c^2)^2$ for $m^2(K\pi)_{high}$. These regions of disagreement are the same observed previously by E687 [11]. We thus conclude that a model with the known $K\pi$ resonances, plus a non-resonant amplitude, is not able to describe the $D^+ \rightarrow K^-\pi^+\pi^+$ Dalitz plot satisfactorily.

A similar pattern – bad fit quality with large NR fraction – is found in the analysis of the decay $D^+ \rightarrow \pi^-\pi^+\pi^+$ when allowing only the established $\pi\pi$ resonances [2]. There we find that the inclusion of an extra scalar resonance improves the fit substantially, giving strong evidence for the $\sigma(500)$. See the section on $D^+ \rightarrow \pi^-\pi^+\pi^+$ below. Thus, we are led to try an extra scalar resonance in our fit model here.

This second fit model, Model B, is constructed by the inclusion of an extra scalar state, with unconstrained mass and width. For consistency, the mass and width of the other scalar state, the $K_0^*(1430)$, are also free parameters of the fit. We adopt a better description for these scalar states by introducing gaussian-type form-factors [12] to take into account the finite size of the decaying mesons. Two extra floating parameters are the meson radii r_D and r_R introduced for these meson sizes.

Using this model, we obtain the values of $797 \pm 19 \pm 42$ MeV/c 2 for the mass and $410 \pm 43 \pm 85$ MeV/c 2 for the width of the new scalar state (first error statistical, second error systematic), referred to here as the κ . The values of mass and width obtained for the $K_0^*(1430)$ are respectively $1459 \pm 7 \pm 6$ MeV/c 2 and $175 \pm 12 \pm 12$ MeV/c 2 , appearing heavier and narrower than presented by the PDG [8]. The decay fractions and relative phases for Model B, with statistical errors, are given in Table 1. Compared to the results of Model A (without κ), the non-resonant mode drops from over 90% to $13 \pm 6\%$. The $\kappa\pi^+$ state is now the dominant channel with decay fraction about 50%. The meson radii r_D and r_R are found to be respectively 5.0 ± 0.5 GeV $^{-1}$ and 1.6 ± 1.3 GeV $^{-1}$, in agreement with values used by other groups [13, 14].

Moreover, the fit quality of Model B is substantially superior to that of Model A. The χ^2/ν is now 0.73 with a CL of 95%. The very good agreement between the model and the data can be seen in the projections of Figure 2(b). A number of studies were done to check these results. They are described in detail in reference [3].

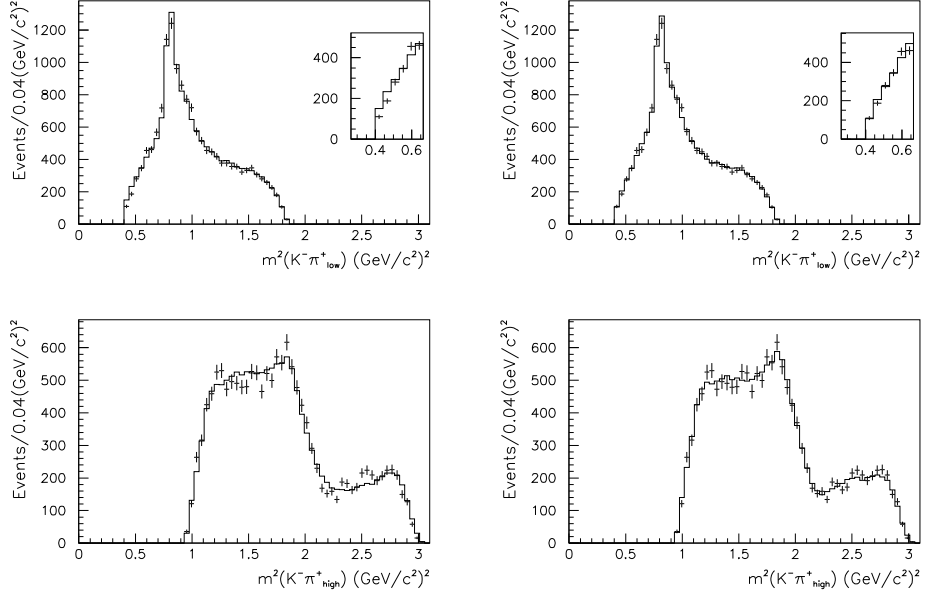


Figure 2: $m^2(K\pi_{\text{low}})$ and $m^2(K\pi_{\text{high}})$ projections for data (error bars) and fast MC (solid line): (a) fit to Model A, without κ , and (b) fit to Model B, with κ .

3 The $D_s^+ \rightarrow \pi^- \pi^+ \pi^+$ Results

In Figure 3 we show the $\pi^- \pi^+ \pi^+$ invariant mass distribution after reconstruction and selection criteria [1, 2] for the sample collected by E791. Besides combinatorial background, reflections from the decays $D^+ \rightarrow K^- \pi^+ \pi^+$, $D^0 \rightarrow K^- \pi^+$ (plus one extra π^+ track) and $D_s^+ \rightarrow \eta' \pi^+$, $\eta' \rightarrow \rho^0(770)\gamma$ are all taken into account. The hatched regions in Figure 3 show the samples used for the Dalitz-plot analyses. There are 1686 and 937 candidate events for D^+ and D_s^+ respectively, with a signal to background ratio of about 2:1. The Dalitz plots for these events are shown in Figure 4, the axes corresponding to the two $\pi^- \pi^+$ invariant-masses squared.

For the $D_s^+ \rightarrow \pi^- \pi^+ \pi^+$ events in Figure 4(a), the signal amplitude includes all channels with well-known dipion resonances [8]: $\rho^0(770)\pi^+$, $f_0(980)\pi^+$, $f_2(1270)\pi^+$, $f_0(1370)\pi^+$, $\rho^0(1450)\pi^+$ and the non-resonant, assumed constant across the Dalitz plot.

For the $f_0(980)\pi^+$ amplitude, instead of a simple Breit-Wigner form, we use a coupled-channel Breit-Wigner function [15],

$$BW_{f_0(980)} = \frac{1}{m_{\pi\pi}^2 - m_0^2 + im_0(\Gamma_\pi + \Gamma_K)} , \quad (1)$$

$$\Gamma_\pi = g_\pi \sqrt{m_{\pi\pi}^2/4 - m_\pi^2}, \quad \Gamma_K = \frac{g_K}{2} \left(\sqrt{m_{\pi\pi}^2/4 - m_{K^+}^2} + \sqrt{m_{\pi\pi}^2/4 - m_{K^0}^2} \right) . \quad (2)$$

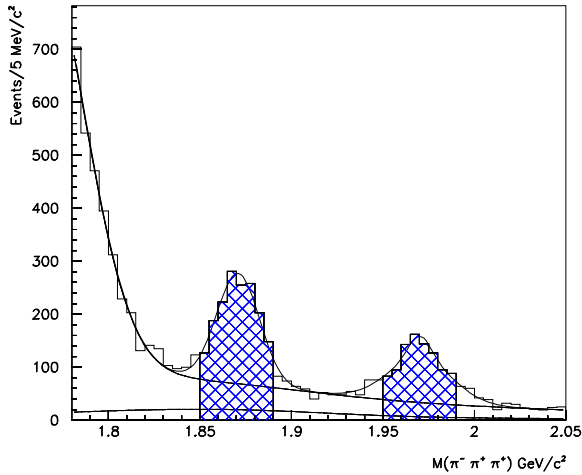


Figure 3: The $\pi^-\pi^+\pi^+$ invariant mass spectrum. The dashed line represent the total background. Events used for the Dalitz analyses are in the hatched areas.

The $D_s^+ \rightarrow \pi^-\pi^+\pi^+$ Dalitz plot is fit to obtain not only the decay fractions and phases of the possible sub-channels, but also the parameters of the $f_0(980)$ state, g_π , g_K , and m_0 , as well as the mass and width of the $f_0(1370)$. The other resonance masses and widths are taken from the PDG[8]. The resulting fractions and phases are given in Table 2. The measured $f_0(980)$ parameters are $m_0 = 977 \pm 3 \pm 2$ MeV/c 2 , $g_\pi = 0.09 \pm 0.01 \pm 0.01$ and $g_K = 0.02 \pm 0.04 \pm 0.03$. By fitting the Dalitz plot using a simple Breit-Wigner function, for the $f_0(980)$ we find $m_0 = 975 \pm 3$ MeV/c 2 and $\Gamma_0 = 44 \pm 2 \pm 2$ MeV/c 2 , and the results for fractions and phases are indistinguishable.

The confidence level of the fit for $D_s^+ \rightarrow \pi^-\pi^+\pi^+$ is 35%. In Figure 5 we show the $\pi^-\pi^+$ mass-squared projections for data (points) and model (solid lines, from fast-MC).

Decay Mode	Fraction (%)	Phase
$f_0(980)\pi^+$	$56.5 \pm 4.3 \pm 4.7$	0° (fixed)
NR	$0.5 \pm 1.4 \pm 1.7$	$(181 \pm 94 \pm 51)^\circ$
$\rho^0(770)\pi^+$	$5.8 \pm 2.3 \pm 3.7$	$(109 \pm 24 \pm 5)^\circ$
$f_2(1270)\pi^+$	$19.7 \pm 3.3 \pm 0.6$	$(133 \pm 13 \pm 28)^\circ$
$f_0(1370)\pi^+$	$32.4 \pm 7.7 \pm 1.9$	$(198 \pm 19 \pm 27)^\circ$
$\rho^0(1450)\pi^+$	$4.4 \pm 2.1 \pm 0.2$	$(162 \pm 26 \pm 17)^\circ$

Table 2: Dalitz fit results for $D_s^+ \rightarrow \pi^-\pi^+\pi^+$.

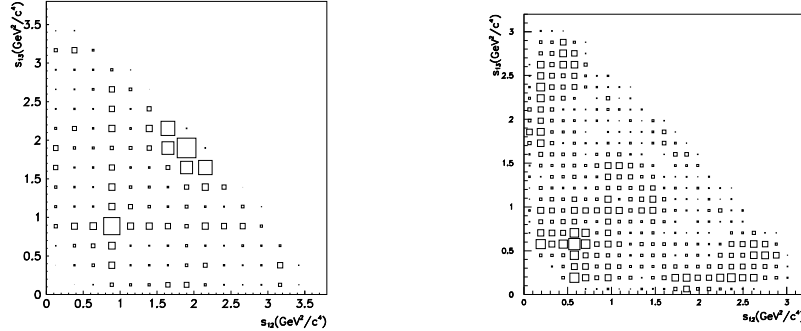


Figure 4: (a) The $D_s^+ \rightarrow \pi^- \pi^+ \pi^+$ Dalitz plot and (b) the $D^+ \rightarrow \pi^- \pi^+ \pi^+$ Dalitz plot. Since there are two identical pions, the plots are symmetrized.

4 The $D^+ \rightarrow \pi^- \pi^+ \pi^+$ Results

In a first approach, we try to fit the $D^+ \rightarrow \pi^- \pi^+ \pi^+$ Dalitz plot of Figure 4(b) with the same amplitudes used for the $D_s^+ \rightarrow \pi^- \pi^+ \pi^+$ analysis. Using this model, the non-resonant, the $\rho^0(1450)\pi^+$, and the $\rho^0(770)\pi^+$ amplitudes are found to dominate, as shown in Table 3, and in agreement with previous reported analyses [16, 17]. However, this model does not describe the data satisfactorily, especially at low $\pi^- \pi^+$ mass squared, as can be seen from Fig. 6(a). The χ^2/ν obtained from the binned Dalitz plot for this model is 1.6, with a CL less than 10^{-5} .

To investigate the possibility that another $\pi^- \pi^+$ resonance contributes to the $D^+ \rightarrow \pi^- \pi^+ \pi^+$ decay, we add an extra scalar resonance amplitude to the signal PDF, with mass and width as floating parameters in the fit.

Decay Mode	Fit without $\sigma(500)\pi^+$		Fit with $\sigma(500)\pi^+$	
	Fraction (%)	Phase	Fraction (%)	Phase
$\sigma(500)\pi^+$	—	—	$46.3 \pm 9.0 \pm 2.1$	$(206 \pm 8 \pm 5)^\circ$
$\rho^0(770)\pi^+$	20.8 ± 2.4	0° (fixed)	$33.6 \pm 3.2 \pm 2.2$	0° (fixed)
NR	38.6 ± 9.7	$(150 \pm 12)^\circ$	$7.8 \pm 6.0 \pm 2.7$	$(57 \pm 20 \pm 6)^\circ$
$f_0(980)\pi^+$	7.4 ± 1.4	$(152 \pm 16)^\circ$	$6.2 \pm 1.3 \pm 0.4$	$(165 \pm 11 \pm 3)^\circ$
$f_2(1270)\pi^+$	6.3 ± 1.9	$(103 \pm 16)^\circ$	$19.4 \pm 2.5 \pm 0.4$	$(57 \pm 8 \pm 3)^\circ$
$f_0(1370)\pi^+$	10.7 ± 3.1	$(143 \pm 10)^\circ$	$2.3 \pm 1.5 \pm 0.8$	$(105 \pm 18 \pm 1)^\circ$
$\rho^0(1450)\pi^+$	22.6 ± 3.7	$(46 \pm 15)^\circ$	$0.7 \pm 0.7 \pm 0.3$	$(319 \pm 39 \pm 11)^\circ$

Table 3: Dalitz fit results for $D^+ \rightarrow \pi^- \pi^+ \pi^+$. First errors are statistical, second systematics (only for fit with $\sigma(500)\pi^+$ mode).

We find that this model improves our fit substantially. The mass and the width of the extra scalar state are found to be $478_{-23}^{+24} \pm 17$ MeV/ c^2 and $324_{-40}^{+42} \pm 21$ MeV/ c^2 ,

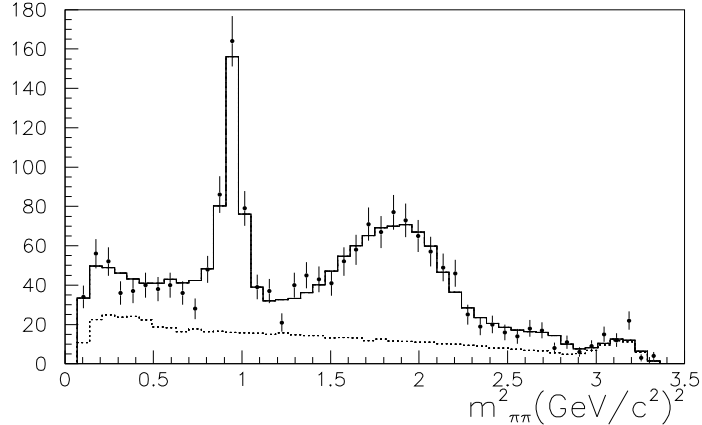


Figure 5: s_{12} and s_{13} ($m_{\pi\pi}^2$) projections for $D_s^+ \rightarrow \pi^-\pi^+\pi^+$ data (dots) and our best fit (solid). The area under the dashed curve corresponds to background.

respectively. Referring to this state as the $\sigma(500)$, we obtain that $\sigma(500)\pi^+$ channel produces the largest decay fraction, as shown in Table 3. The non-resonant amplitude, which is dominant in the model without $\sigma(500)\pi^+$, drops substantially. This model describes the data much better, as can be seen by the $\pi\pi$ mass squared projection in Fig. 6(b). The χ^2/ν is now 0.9, with a corresponding confidence level of 91%.

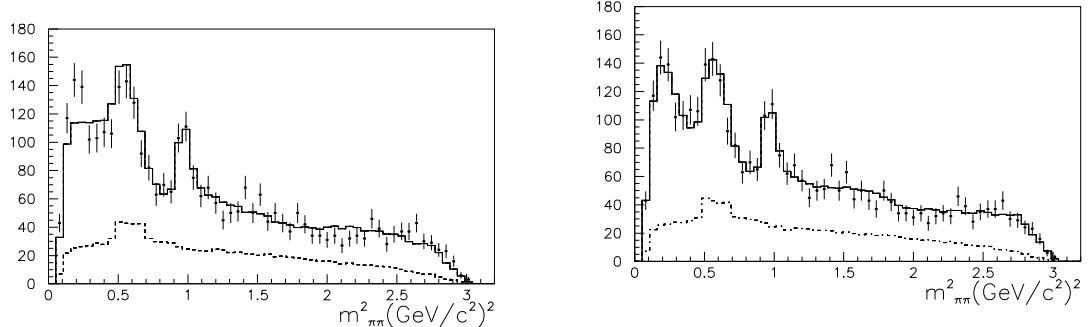


Figure 6: s_{12} and s_{13} ($m_{\pi\pi}^2$) projections for $D^+ \rightarrow \pi^-\pi^+\pi^+$ data (dots) and our best fit (solid) for models (a) without and (b) with $\sigma(500)\pi^+$ amplitude. The dashed distributions corresponds to the expected background levels.

5 Conclusion

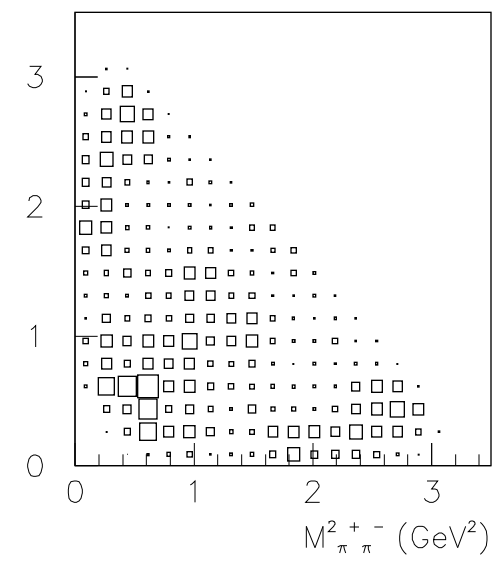
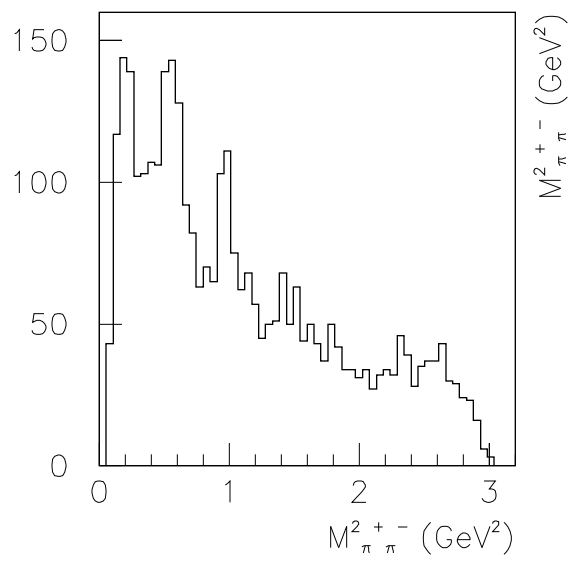
From the data of the Fermilab E791 experiment, we studied the Dalitz plots of the decays $D^+ \rightarrow K^-\pi^+\pi^+$, $D_s^+ \rightarrow \pi^-\pi^+\pi^+$ and $D^+ \rightarrow \pi^-\pi^+\pi^+$. In these three final states, the scalar intermediate resonances were found to give the main contribution to the decay rates. We obtained strong evidence for the existence of $\sigma(500)$ and κ scalar mesons, measuring their masses and widths. We also obtained new measurements for masses and widths of the other scalars studied, $f_0(980)$, $f_0(1430)$ and $K_0^*(1430)$.

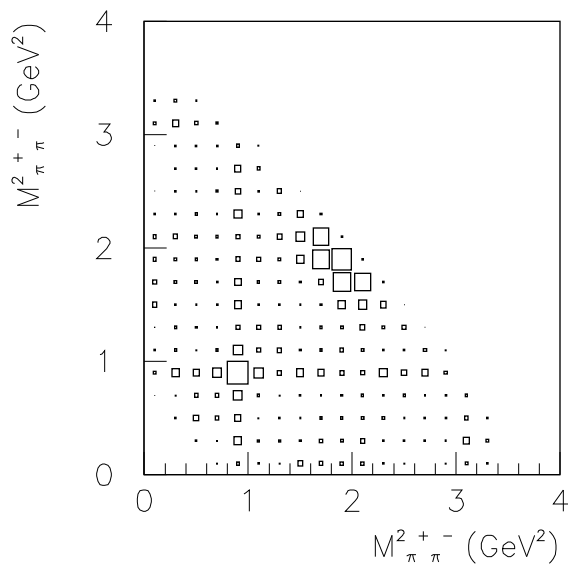
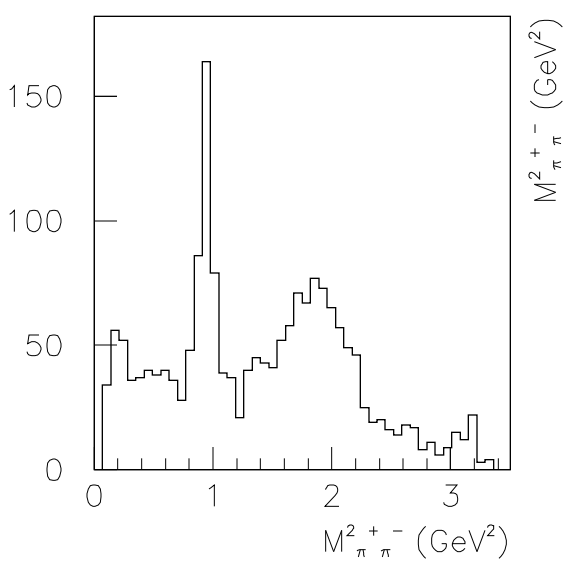
The results presented here show the potential of D meson decays for the study of light meson spectroscopy, in particular in the scalar sector.

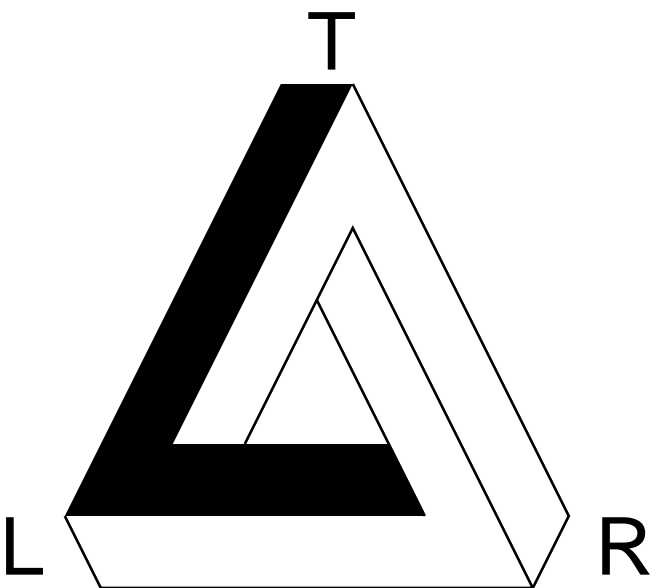
References

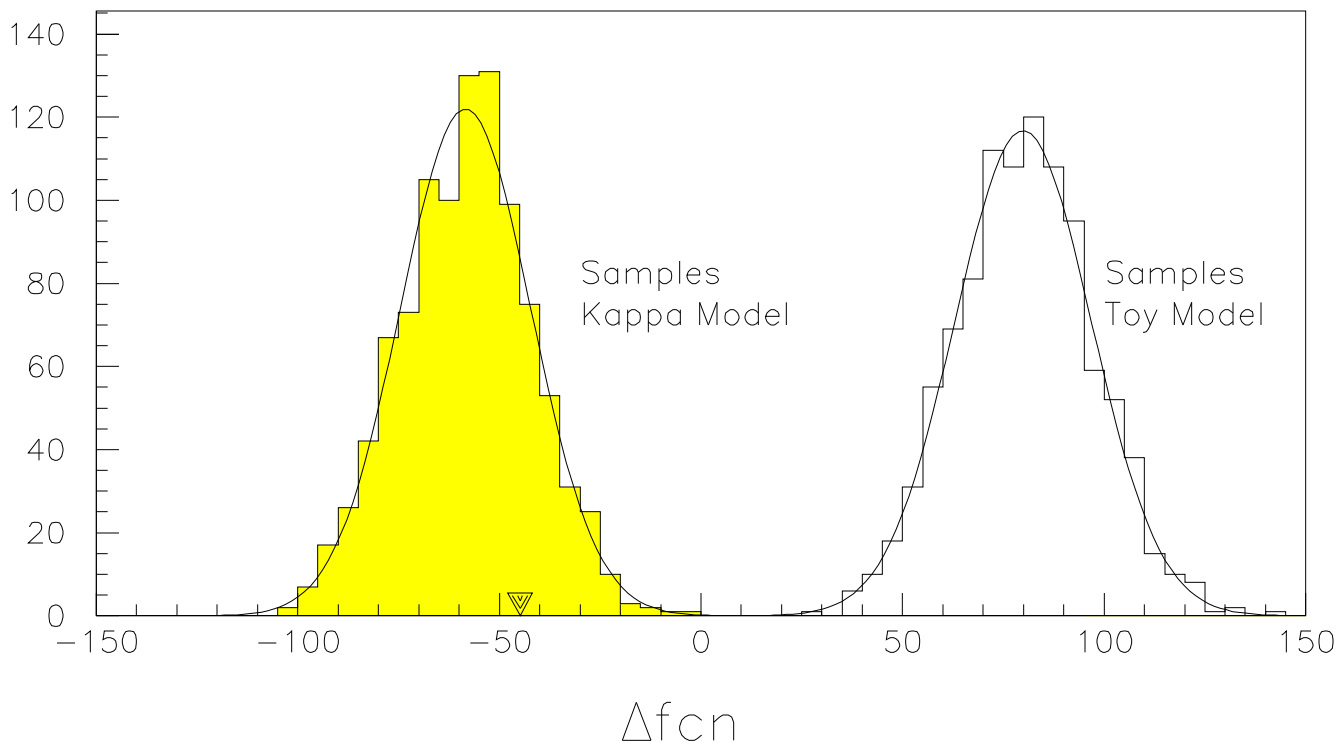
- [1] E791 Collaboration, E.M. Aitala *et al.*, Phys. Rev. Lett. **86**, 765 (2001).
- [2] E791 Collaboration, E.M. Aitala *et al.*, Phys. Rev. Lett. **86**, 770 (2001).
- [3] C. Göbel, in *Proceedings of Heavy Quarks at Fixed Target*, Frascati Physics Series Vol. XX (Laboratory Nazionali de Frascati, Frascati (Roma), Italy, 2001), p. 373, edited by I.Bediaga, J. Miranda and A. Reis, hep-ex/0012009. And E791 Collaboration, E.M. Aitala *et al.* hep-ex/0204018, submitted to Phys. Rev. Lett.
- [4] J.A. Appel, Ann. Rev. Nucl. Part. Sci. **42**, 367 (1992); D. Summers *et al.*, hep-ex/0009015; S. Amato *et al.*, Nucl. Instr. Meth. A **324**, 535 (1993); E791 Collaboration, E.M. Aitala *et al.*, Eur. Phys. J. direct C **4**, 1 (1999). S. Bracker *et al* IEEE Trans. Nucl. Sci **43**, 2457 (1996).
- [5] WA102 Collaboration, D. Barberis, *et al.* Phys. Lett. B **453**, 316 (1999).
- [6] CLEO Collaboration, D.M. Asner *et al.*, Phys Rev D **61**, 012002 (2000)
- [7] GAMS Collaboration, D. Alde, *et al.*, Phys. Lett. B **397**, 350 (1997).
- [8] Particle Data Group, D.E. Groom *et al.* Eur. Phys. Jour. C **15**, 1 (2000).
- [9] N. Törnqvist and A.D. Polosa, in *Proceedings of Heavy Quarks at Fixed Target*, Frascati Physics Series Vol. XX (Laboratory Nazionali de Frascati, Frascati (Roma), Italy, 2001), p. 385 edited by I.Bediaga, J. Miranda and A. Reis, hep-ph/0011107. And F.E. Close and N. Törnqvist, hep-ph/0204205.
- [10] E691 Collaboration, J.C. Anjos *et al.*, Phys. Rev. D **48**, 56 (1993).
- [11] E687 Collaboration, P.L. Frabetti *et al.*, Phys. Lett. B **331**, 217 (1994).

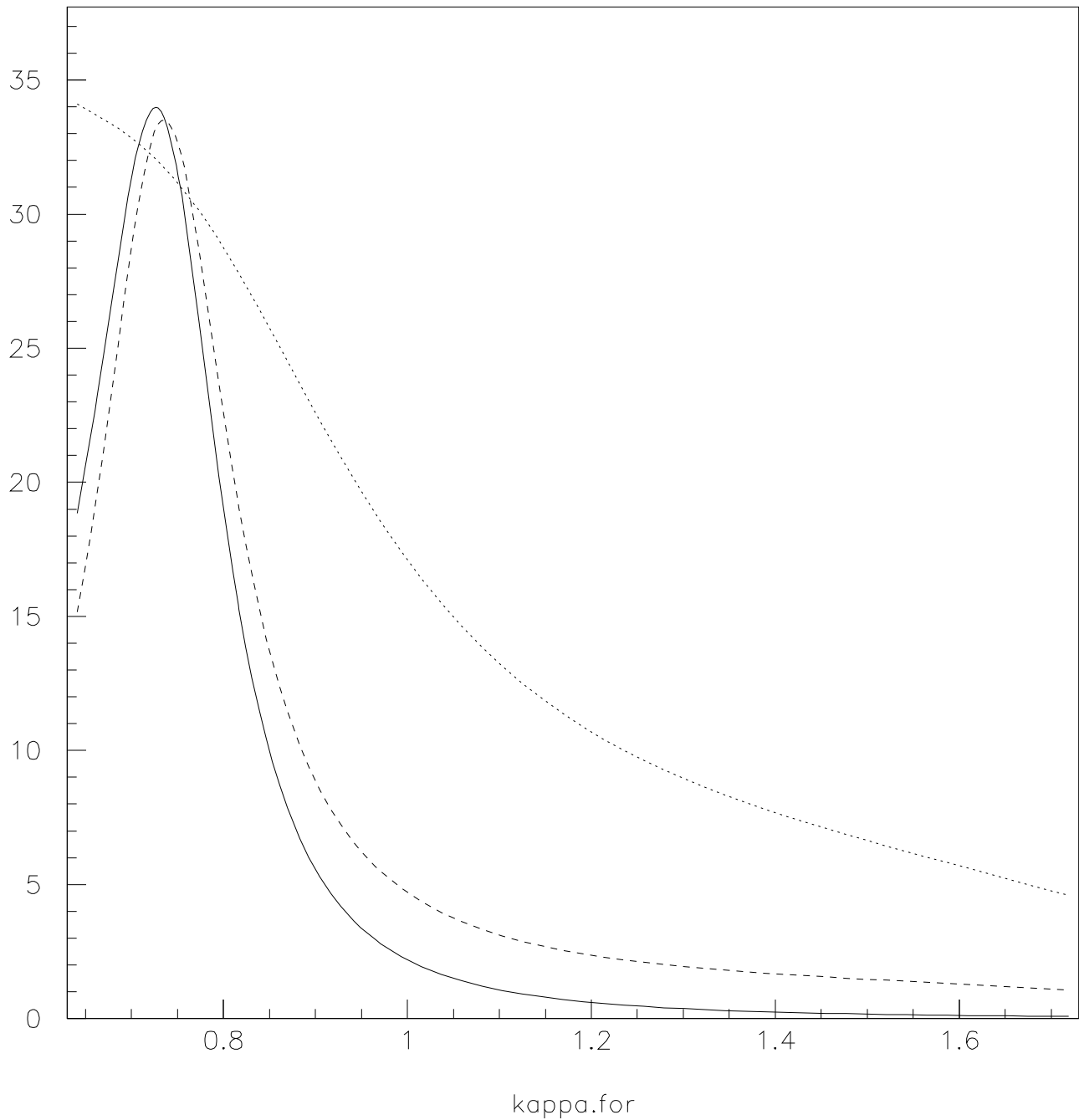
- [12] N.A. Törnqvist, Z. Phys. C **68**, 647 (1995).
- [13] ARGUS Collaboration, H. Albrecht *et al.*, Phys. Lett. B **308**, 435 (1993).
- [14] CLEO Collaboration, S. Kopp *et al.*, Phys. Rev. D **63**, 092001 (2001).
- [15] WA76 Collaboration, T.A. Armstrong *et al.*, Z. Phys. C **51**, 351 (1991).
- [16] E691 Collaboration, J.C. Anjos *et al.*, Phys. Rev. Lett. **62**, 125 (1989).
- [17] E687 Collaboration, P.L. Frabetti *et al.*, Phys. Lett. B **407**, 79 (1997).

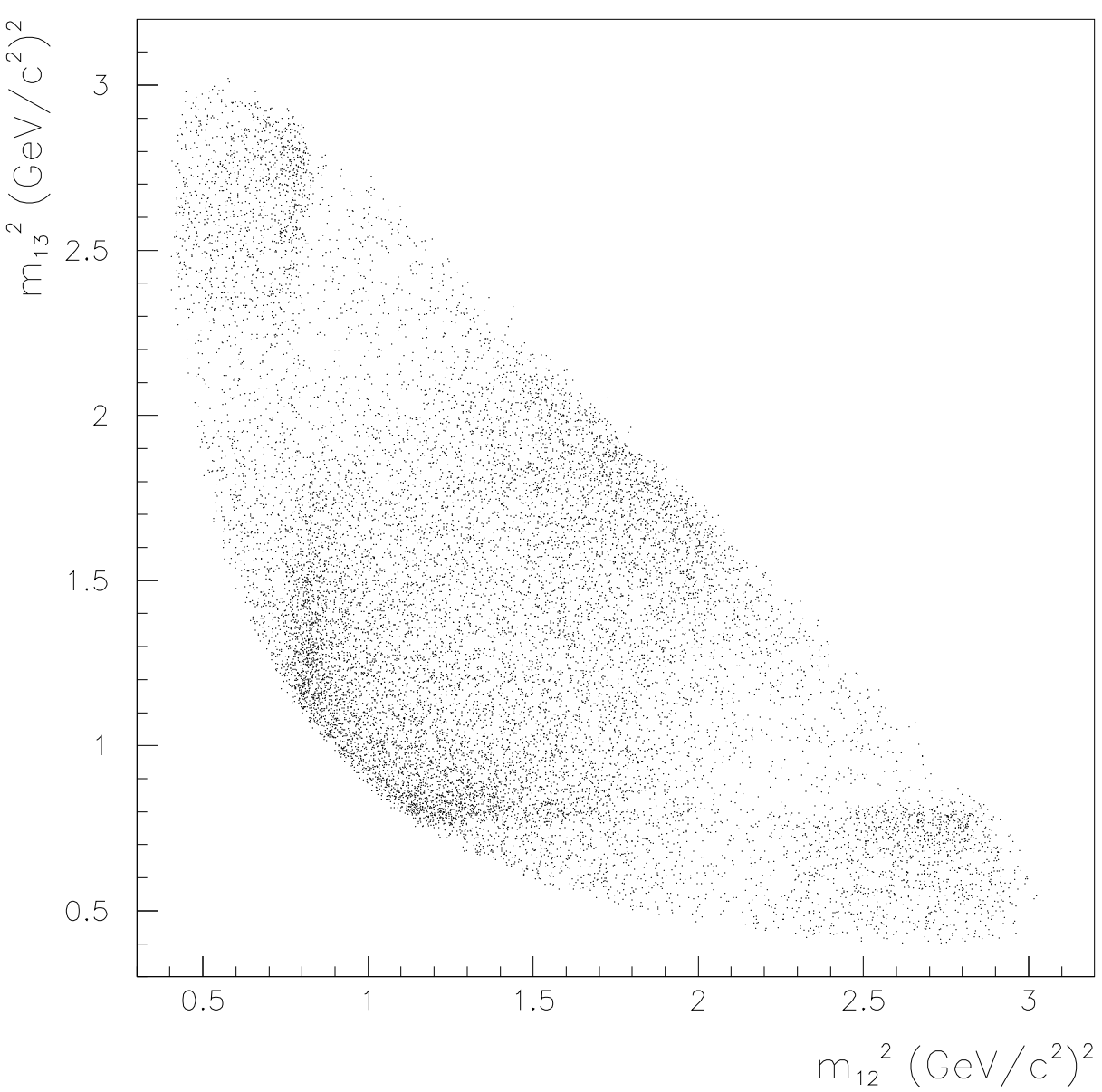












The L^AT_EX Companion